FOREX Publication
Open Access | Rapid and quality publishing

International Journal of
Electrical and Electronics Research (IJEER)
Research Article | Volume 11, Special Issue NGWCN | Pages 25-32 | e-ISSN: 2347-470X

Fractal Cross-Slot-Coupled Antenna with Dielectric Resonator Elements having Circular Polarization

Pedada Krishna Rao[1*], M. Satya Anuradha[2], and V. Rajya Lakshmi[3]

[1*]*Research Scholar, Department of ECE, Andhra University, Visakhapatnam, India; Email: krishnapedada.r@gmail.com*
[2]*Professor, Department of ECE, Andhra University, Visakhapatnam, India; Email: satyaanuradham@gmail.com*
[3]*Professor, Department of ECE, ANITS, Visakhapatnam, India; Email: rajyalakshmiv87@gmail.com*

***Correspondence:** Pedada Krishna Rao; krishnapedada.r@gmail.com

ABSTRACT- This article presents the design and analysis of an "ultra-wideband (UWB)" Fractal Cross-slot-Coupled Antenna with "Dielectric Resonator Elements (DREs)" exhibiting circular polarization and band-notched characteristics. The proposed antenna aims to reject the frequency range of 5.1 GHz to 5.9 GHz while maintaining high impedance bandwidth and radiation efficiency. A coplanar waveguide feeds the planar UWB antenna, featuring a narrow slot on the radiating element and a dielectric resonator mounted on top. Simulation results demonstrate excellent performance in terms of impedance bandwidth and radiation efficiency. To further improve the design for wireless applications, Fractal-slot-aperture coupled DRE antennas are employed. The proposed configuration takes into account the radiative efficiency and concomitant excitation of the rectangular DRE by a "Circularly Polarized Dielectric Resonator Antenna (CPDRA)" coupled through a fractal cross-slot. By appropriately adjusting the fractal cross-slot size, a wider "axial ratio (AR)" bandwidth is achieved through the combination of its resonance with the dielectric resonator. The antenna is designed utilizing the proposed fractal cross-slot-coupled CPDRA, with its architecture and efficiencies thoroughly investigated. The performance of the proposed antenna demonstrates its potential for various wireless communication applications, highlighting the advantages of integrating Fractal Cross-slot-coupled DREs in antenna design.

Keywords: Ultra-wideband, Circular polarization, Fractal cross-slot, Micro-strip antenna, Return-loss, Radiation pattern, and Axial-ratio.

ARTICLE INFORMATION

Author(s): Pedada Krishna Rao, M. Satya Anuradha, and V. Rajya Lakshmi;

Received: 23/07/2023; **Accepted**:14/09/2023; **Published**: 30/12/2023;
E- ISSN: 2347-470X;
Paper Id: IJEER NG-WCN-017;
Citation: 10.37391/IJEER.11ngwcn05
Webpage-link:
https://ijeer.forexjournal.co.in/archive/volume-11/ijeer-11ngwcn05.html

Publisher's Note: FOREX Publication stays neutral with regard to jurisdictional claims in Published maps and institutional affiliations.

1. INTRODUCTION

Fractal antennas offer benefits like low cost, easy integration, and small size. They use a flat micro-strip shape and can reduce size by up to four times while performing well, with potential for multiband performance. Dielectric Resonator Antennas (DRAs) are gaining traction due to their excellent radiation efficiency and minimal surface wave loss. They can be fed in various ways, such as micro-strip line feed and coaxial probe feed.

Initially, DRA research centered on linearly polarized devices. The first Circularly Polarized DRA (CPDRA) was developed by modifying a rectangular-DRA. Subsequent CPDRA designs have evolved, with the array element and feeding network affecting performance. Multiple techniques have been proposed to enhance the axial-ratio bandwidth of a standalone DRA, but these aren't always suitable for DRA arrays due to complications like complex feeding networks or reduced radiation efficiency.

Introducing a fractal cross slot into the ground plane beneath the resonator achieves an efficient axial-ratio bandwidth for a specific CP rectangular DRA element. This design is straightforward and avoids multiple feeds or layered substrates. A prototype of this antenna was built, and its results were compared with simulations.

2. DESIGN OF THE DRA ANTENNA

The band-notched UWB antenna has a radiating patch composed of circular and semi-circular structures. Adjusting the antenna's current distribution enables it to operate in the ultra-wideband spectrum. The ideal match requires adjusting the coplanar waveguide distance (s_{o2})to an optimal value, with the best resonance observed at $s_{o2} = 0.2mm$as shown in *figure 1*.

The radiation patch consists of overlapping semicircles and circles. Modifying the circle's diameter and the semicircular reflector's radius ensures the antenna's operation within the ultra-wideband. Figure 1 also indicates a noticeable decrease in the reflection-coefficient as the frequency spectrum from 5.9GHz to 11.8GHz increases, with peak resonance at $a = 8.2mm$.

FOREX Publication
Open Access | Rapid and quality publishing
International Journal of Electrical and Electronics Research (IJEER)
Research Article | Volume 11, Special Issue NGWCN | Pages 25-32 | e-ISSN: 2347-470X

Antenna design: *Figure 1* presents the antenna's structure. It uses a Rogers RT/TR 5880 substrate with a permittivity of $r = 2.2$, a loss tangent of 0.0009, and a 0.508mm thickness, sized 50mm x 50mm. A fractal cross-slot is carved on the ground, beneath a central ceramic cube (permittivity $r = 8.9$, 9.8mm x 9.8mm x 9.1mm). The 50 micro-strip line on the substrate's bottom has lengths $l_{f1} + l_{f2}$ and width wf. $l_{f1}$is the distance from the 50 ports to the cube's center, and $l_{f2}$from the cube's center to the microstrip line's end.

The band-notched UWB antenna's patch features circular and semi-circular shapes tailored for ultra-wideband operation by adjusting its current distribution. Ideal impedance matching necessitates tuning the coplanar waveguide distance, best at $s_{o2} = 0.2mm$as shown in *figure 1*. The patch has overlapping semicircles and circles. Modifying the circle's diameter and semicircular reflector's radius optimizes operation. *Figure 1* indicates that as the 5.9GHz to 11.8GHz frequency reflection coefficient rises, it drops sharply, peaking at $a = 8.2mm$.

Substrate: The antenna's foundational layer is the substrate. It affects radiation efficiency, bandwidth, and size. This design employs the Rogers RT/duroid 5880 substrate due to its low dielectric loss tangent, enhancing antenna performance. Its dimensions are 50mm x 50mm x 0.508mm, with a relative permittivity of ($\varepsilon r = 2.2$).

Radiating Element: The radiating element emits and receives electromagnetic waves. This design's radiating patch consists of overlapping circles and semicircles. Adjusting the circle diameter *(a)* and semicircular reflector *(b)* ensures optimal ultra-wideband performance. For ideal operation, the diameters for *a* and *b* are 8.2mm and 12.2mm, respectively.

Fractal Cross-Slot: Essential for impedance matching and bandwidth enhancement, the fractal cross-slot is carved on the ground plane beneath a central ceramic cube (9.8mm x 9.8mm x 9.1mm, permittivity $\varepsilon r = 8.9$). The fractal design arises from iterative processes based on standard cross-slots, with iterations affecting slot dimensions.

Fractal Cross-Slot's Impact: These structures influence resonance and bandwidth. Adjusting the cross-slot through iterative processes impacts impedance matching and performance. By manipulating the length coefficient and constant iterative angle, a broader axial ratio bandwidth in the ultra-wideband is achieved. *Figure 1* and *tables 1, 2* showcase structures for $(n = 0,1, and 2)$iterations. The foundation for the fractal structure is standard cross-slots with lengths l_{s1}, $l_{s1}(l_{s2} = k_s l_{s1})$ and width ws. Iterations involve a constant angle φ with a length coefficient of 0.5, while slot width remains unchanged.

Coplanar Waveguide: This feeding structure supplies power to the antenna. The 50-ohm microstrip line ensures power transfer with good impedance matching. The line's dimensions, length $(l_{f1} + l_{f2})$and width (wf), are crucial, with an optimal coplanar waveguide distance $(s_{o2})$of 0.2mm for best impedance matching.

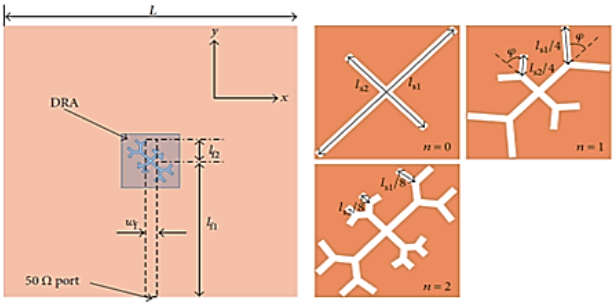

Figure 1: The geometry of the proposed antennas

Table 1: Specifications table of *fig .1*

W_2	L_2	W_{f2}	l_{12}	A	b
28	26	1.5	3	8.2	12.2
N	L_{o2}	S_{o2}	h	M	
0.2	10.3	0.2	1.6	15	

Table 1: specifications table of *fig. 1*

Component	Variables	Value(mm)
Substrate	$W \times L \times H, \epsilon r$	50×50×1.6, 4.4
Fractal Slot	$l_{s1}, l_{s2}, k_s, \varphi, W_s$	9.7, 5.529, 0.57, 40 deg, 0.4
Feed Line	l_{f1}, l_{f2}, Wf	25, 4, 1.52
DRA	$W \times L \times H$	13x10x5

3. SIMULATION USING HFSS

High-Frequency Structure Simulator (HFSS) is a leading full-wave electromagnetic (EM) field simulator, utilizing Windows' graphical interface. It seamlessly combines simulation, solid modeling, and visualization to offer accurate solutions to complex 3D EM issues. For our band-notched UWB antenna design with circular polarization, we employed HFSS. HFSS uses the Finite Element Method (FEM) for a precise representation of the antenna and its environment. Its adaptive meshing feature adjusts the mesh in rapid EM field fluctuation areas, enhancing accuracy and reducing numerical errors. HFSS visuals aid in understanding radiation patterns and spotting design imperfections. It computes essential antenna properties like S-parameters, resonance frequency, and VSWR. Ansoft Corporation, HFSS's developer, revolutionized EM simulation using FEM. In our research, using HFSS, we simulated the proposed UWB antenna and validated the design against experimental findings, ensuring it meets performance criteria for wireless communication.

4. SIMULATION RESULTS

4.1 Fractal slot of the 0th iteration-coupled DRA element in a CPDRA

FOREX Publication
Open Access | Rapid and quality publishing
International Journal of Electrical and Electronics Research (IJEER)
Research Article | Volume 11, Special Issue NGWCN | Pages 25-32 | e-ISSN: 2347-470X

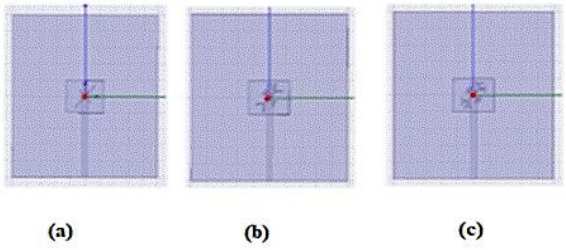

Figure 2: Fractal Cross-Slot-Coupled DRA Elements in a High-Frequency Synthesis-Solution-designed CPDRA.

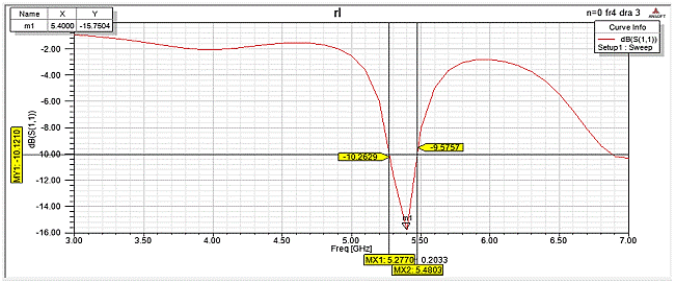

Figure 3: The return loss of a CPDRA with a zeroth-iteration Fractal Cross-Slot DRA.

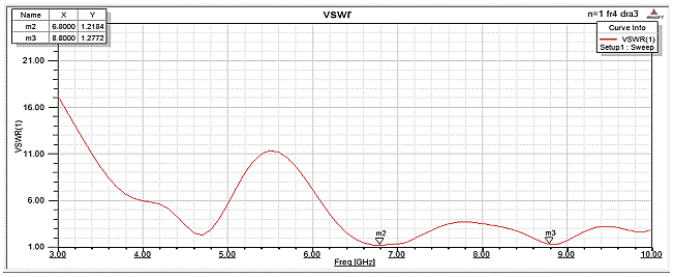

Figure 4: VSWR for CPDRA having Fractal Cross-Slot of "DRA with zeroth iteration"

Figure 2(a) displays the CPDRA with a fractal cross-slot with zero iterations, while its HFSS-simulated return loss is presented in *figure 3*. At 5.4 GHz, the return loss is -15 dB, suggesting a good impedance match. The bandwidth between 5.2 GHz and 5.48 GHz has a return loss under -10 dB, suitable for many uses. The VSWR, which measures impedance matching, is shown in *figure 4*. Ideal VSWR values lie between 1 and 2. For this antenna at 5.4 GHz, the VSWR is 1.3898, denoting a good impedance match.

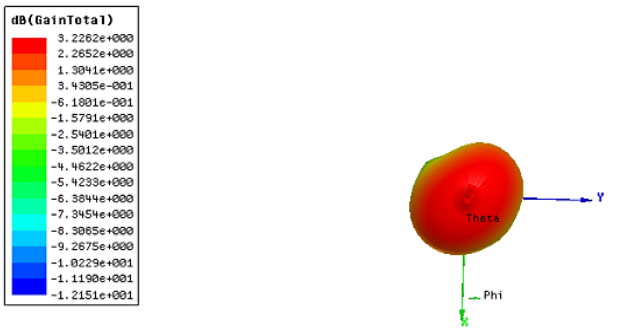

Figure 5: (a) Gains of CPDRA having Fractal Cross-Slot of "DRA with zeroth iteration"

Figure 5(a) and 5(b) show the 3-D gains of the CPDRA with a fractal cross-slot, corresponding to *figure 2(a)*. Typically, antennas should have gains over 3 dB. This design has a gain of 3.22 dB.

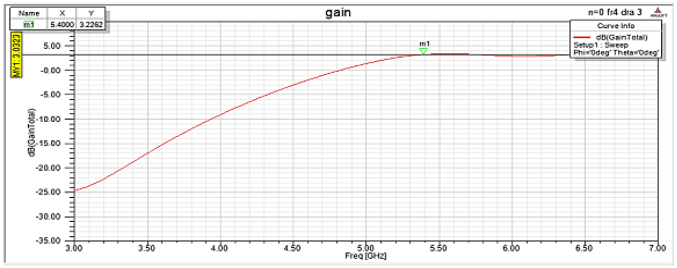

Figure 5: (b) Gain vs frequency plot of CPDRA having Fractal Cross-Slot of "DRA with zeroth iteration".

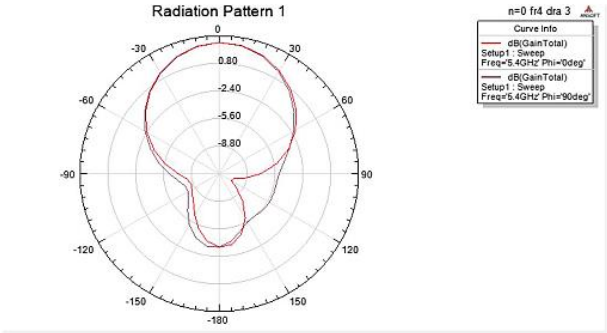

Figure 6: Radiation pattern of CPDRA having Fractal Cross-Slot of "DRA with zeroth iteration".

The radiation pattern of an antenna depicts the power variation based on direction. This variation is observed at different arrival angles in the antenna's far-field. *Figure 6* displays the radiation pattern of the CPDRA with a fractal cross-slot, as simulated by HFSS.

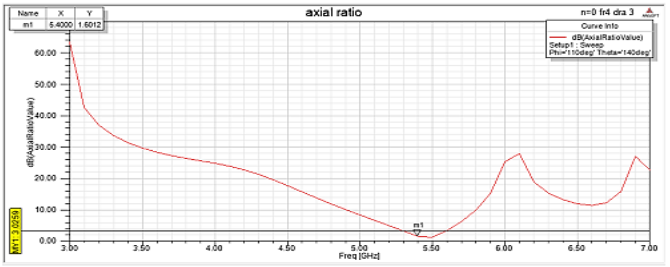

Figure 7: Axial Ratio of CPDRA having Fractal Cross-Slot of "DRA with zeroth iteration".

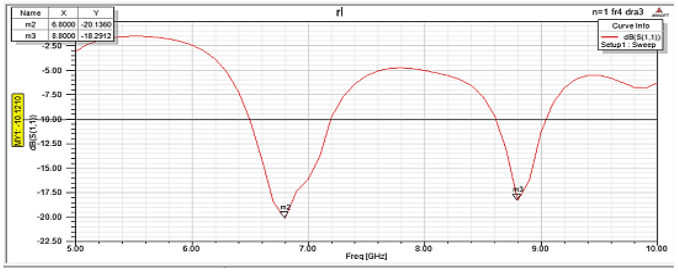

Figure 8: The return loss of CPDRA having Fractal Cross-Slot of "DRA with First iteration"

FOREX Publication
Open Access | Rapid and quality publishing
International Journal of Electrical and Electronics Research (IJEER)
Research Article | Volume 11, Special Issue NGWCN | Pages 25-32 | e-ISSN: 2347-470X

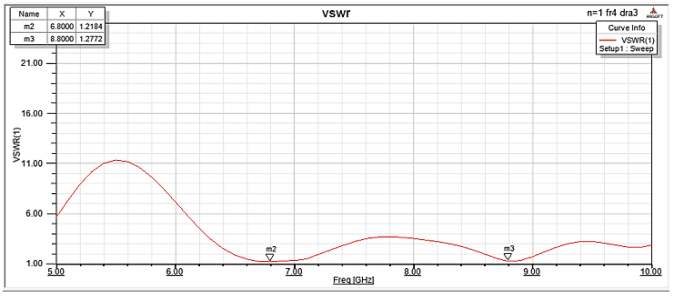

Figure 9: VSWR for CPDRA having Fractal Cross-Slot of "DRA with First iteration"

The "axial ratio (AR)" represents the ratio between the major and minor axes of a polarization ellipse. For a CPDRA, values close to 0 dB are ideal, but below 3 dB is typically acceptable. *Figure 7* shows the axial ratio of the CPDRA with a fractal cross-slot, as simulated by HFSS, corresponding to *figure 2(a).*

4.2 CPDRA having fractal cross-slot of "DRA with first iteration"

Figure 8 shows the return loss for the first iteration CPDRA with a fractal cross-slot, referencing *figure 2(b).* The losses are -20.136 dB at 6.8 GHz and -18.2912 dB at 8.8 GHz. For an ideal match, the Voltage Standing Wave Ratio (VSWR) should be at least unity. *Figure 9* displays the VSWR of the CPDRA with a first iteration fractal cross-slot, referencing *figure 2(b).* Practical VSWR values lie between 1 and 2. For this antenna, they are 1.2184 at 6.8 GHz and 1.2772 at 8.8 GHz.

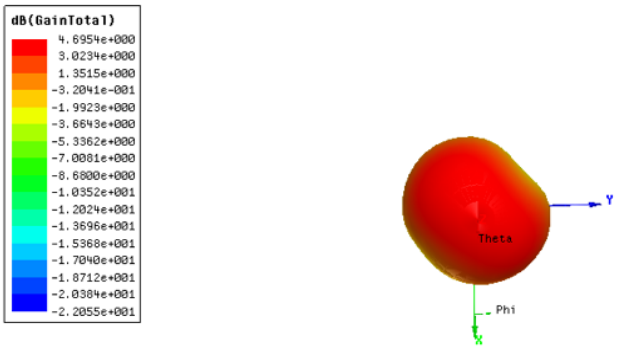

(a)

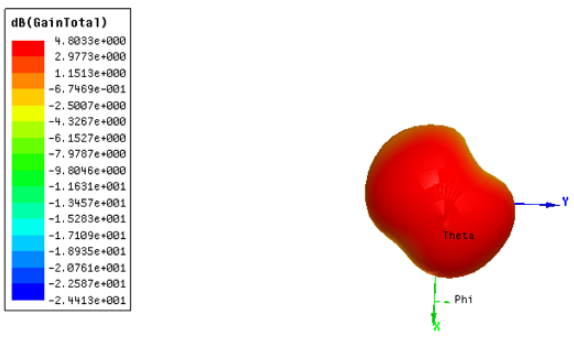

(b)

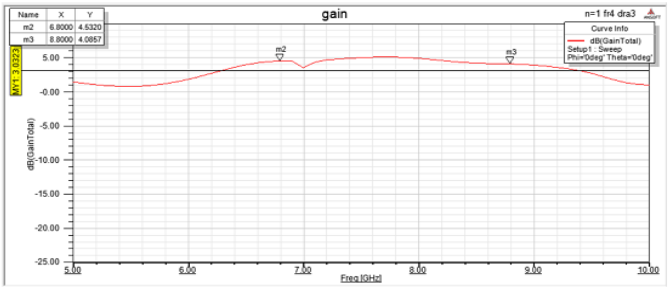

(c)

Figure 10: (a) The gain for CPDRA having Fractal Cross-Slot of "DRA with First iteration" at 6.8GHz, (b) The gain for CPDRA having Fractal Cross-Slot of "DRA with First iteration" at 8.8GHz, (c) Gain vs frequency plot for CPDRA having Fractal Cross-Slot of "DRA with First iteration"

Figures 10(a-c) illustrate the 3D gain of this CPDRA. Typically, antennas should have gains over 3 dB. This design achieves gains of 4.69 dB at 6.8 GHz and 4.8 dB at 8.8 GHz.

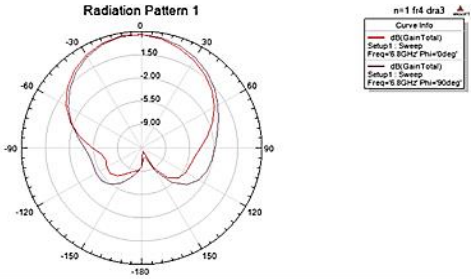

(a)

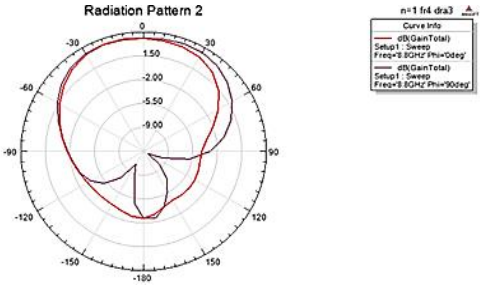

(b)

Figure 11: (a) The radiation pattern of CPDRA having Fractal Cross-Slot of "DRA with First iteration" at 6.8GHz, (b) The radiation pattern of CPDRA having Fractal Cross-Slot of "DRA with First iteration" at 8.8GHz

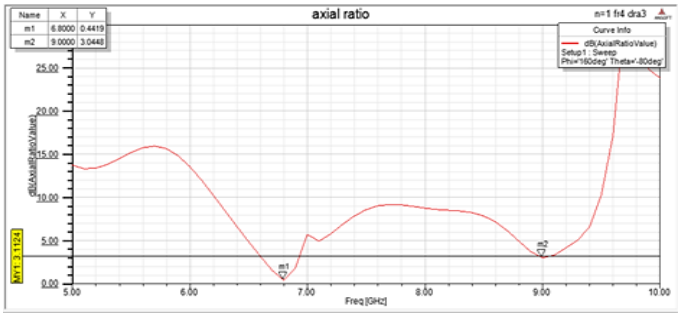

Figure 12: Axial Ratio of CPDRA having Fractal Cross-Slot of "DRA with First iteration".

FOREX Publication
Open Access | Rapid and quality publishing
International Journal of Electrical and Electronics Research (IJEER)
Research Article | Volume 11, Special Issue NGWCN | Pages 25-32 | e-ISSN: 2347-470X

The radiation pattern shows the antenna's power variation based on its orientation. *Figures 11(a-b)* display the radiation pattern for the first iteration CPDRA with a fractal cross-slot, referencing *figure 2(b)*. The axial ratio (AR) measures the ratio between the minor and major axes of the polarization ellipse. For a CPDRA, a value closer to 0 dB is ideal, but values below 3 dB are common. *Figure 12* shows the axial ratio for the first iteration, matching *figure 2(b)*.

4.3 Simulation results of CPDRA having Fractal Cross-Slot of "DRA with second iteration"

Figure 13 presents the return loss of the (CPDRA) with a fractal cross-slot for the second iteration, as simulated in the (HFSS) and corresponding to *figure 2(c)*. The return loss is shown to be -28.9154 dB at 6.4 GHz and -15.7388 dB at 8.4 GHz. For an ideal match, the VSWR should be at least unity.

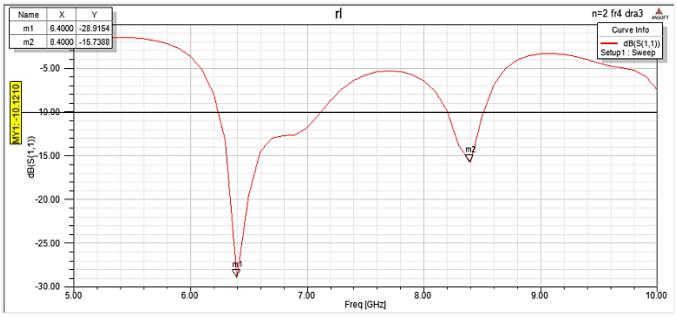

Figure 13: The return loss for CPDRA having Fractal Cross-Slot of "DRA with second iteration"

Figure 14 shows the VSWR for the CPDRA with a fractal cross-slot in its second iteration, corresponding to *figure 2(c)*. Practical antennas have a VSWR between 1 and 2. For this design, the VSWR is 1.0743 at 6.4 GHz and 1.3904 at 8.4 GHz.

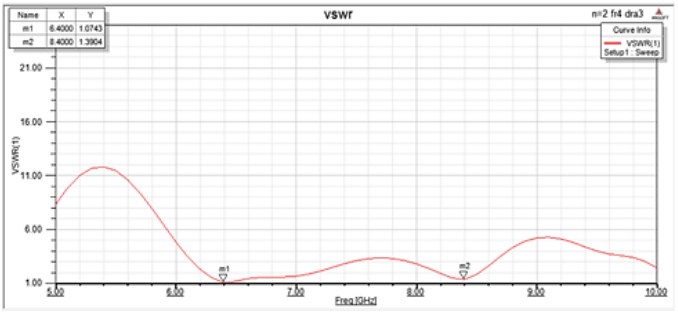

Figure 14: The VSWR for CPDRA having Fractal Cross-Slot of "DRA with second iteration"

Figures 15(a-c) show the 3D gains of the second iteration CPDRA with a fractal cross-slot, referencing *figure 2(c)*. Antennas ideally should have gains over 3 dB. This antenna registers gains of 4.14 dB at 6.4 GHz and 5.85 dB at 8.4 GHz.

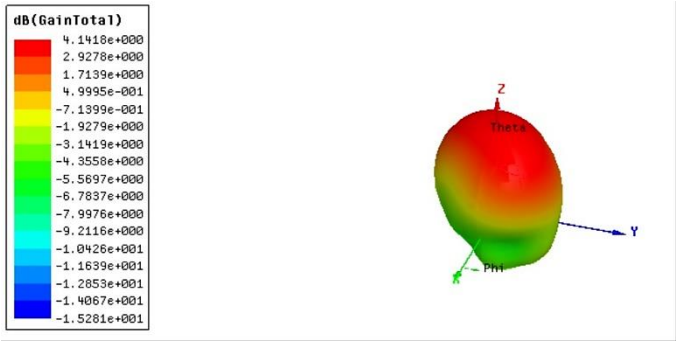

(a)

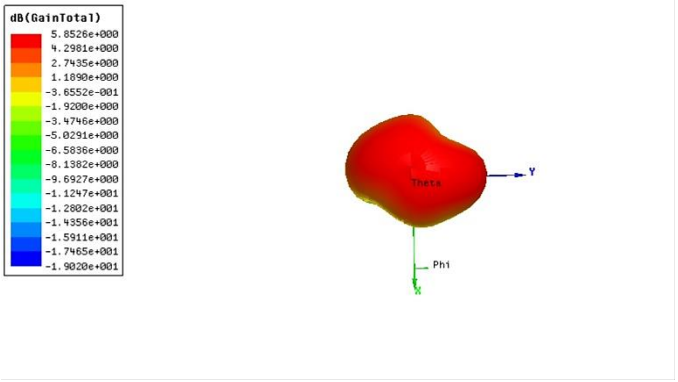

(b)

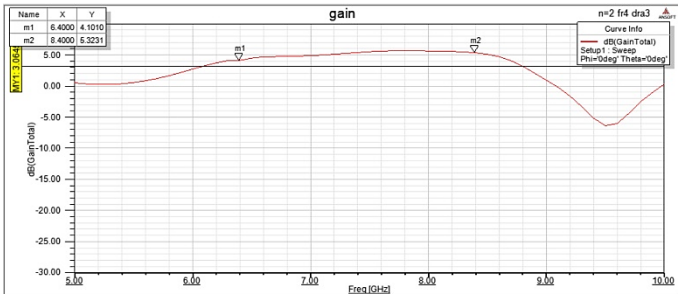

(c)

Figure 15: (a). The gains for CPDRA having Fractal Cross-Slot of "DRA with second iteration" at 6.4GHz, (b). Gains for CPDRA having Fractal Cross-Slot of "DRA with second iteration" at 8.4GHz, (c). Gains vs frequencies plot for CPDRA having Fractal Cross-Slot of "DRA with second iteration"

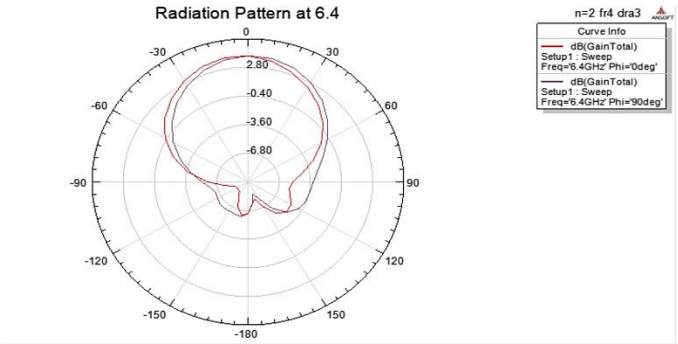

(a)

FOREX Publication
Open Access | Rapid and quality publishing
International Journal of Electrical and Electronics Research (IJEER)
Research Article | Volume 11, Special Issue NGWCN | Pages 25-32 | e-ISSN: 2347-470X

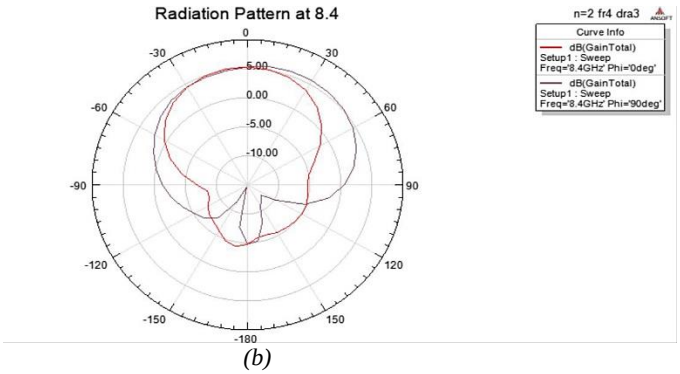

(b)

Figure 16: (a). The RP (radiation-pattern) of CPDRA having Fractal Cross-Slot of "DRA with second iteration" at 6.4 GHz, (b). The RP (radiation-pattern) of CPDRA having Fractal Cross-Slot of "DRA with second iteration" at 8.4 GHz.

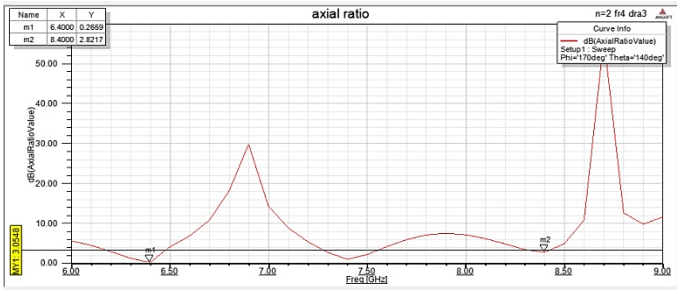

Figure 17: AR (Axial-Ratio) of CPDRA having Fractal Cross-Slot of "DRA with second iteration"

The radiation pattern shows how an antenna distributes power in various directions, observed in its far-field region. *Figures 16(a) and 16(b)* illustrate the pattern of the CPDRA with a second iteration fractal cross-slot, based on HFSS simulations, relating to *figure 2(c).* The axial ratio (AR) represents the polarization ellipse's major to minor axis ratio. For a circularly polarized antenna, an AR near 0 dB is ideal, but values below 3 dB are commonly accepted. *Figure 17* presents the AR for the same CPDRA, corresponding to *figure 2(c).*

4.4 Fabrication model

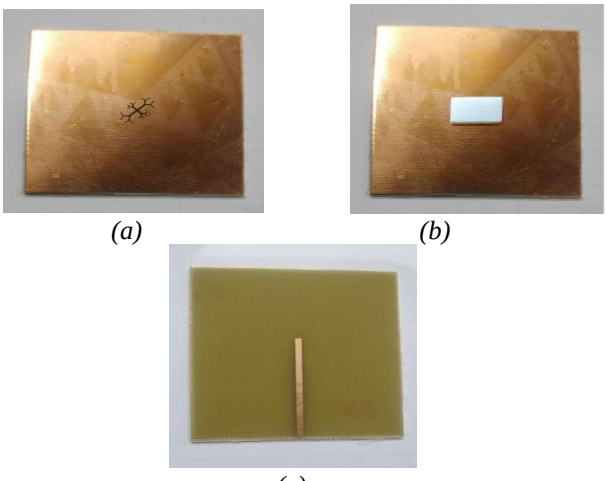

(a) *(b)*

(c)

Figure 18: Fabricated Antenna (a) Front View without DRA, (b) Front View with DRA, (c) Back View

Figure 19: Experimental setup (a) without DRA, (b) with DRA

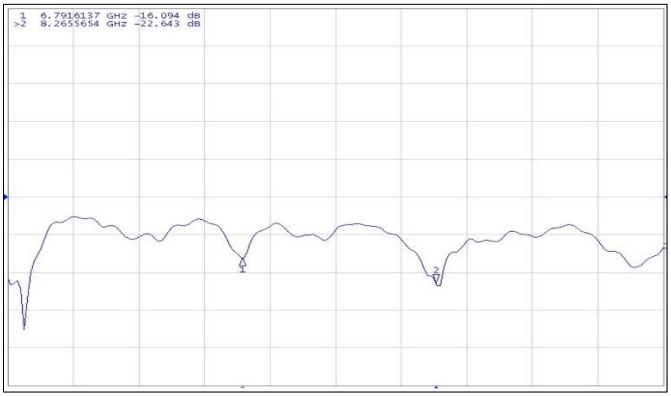

Figure 20: return-loss of fabricated antenna without DRA

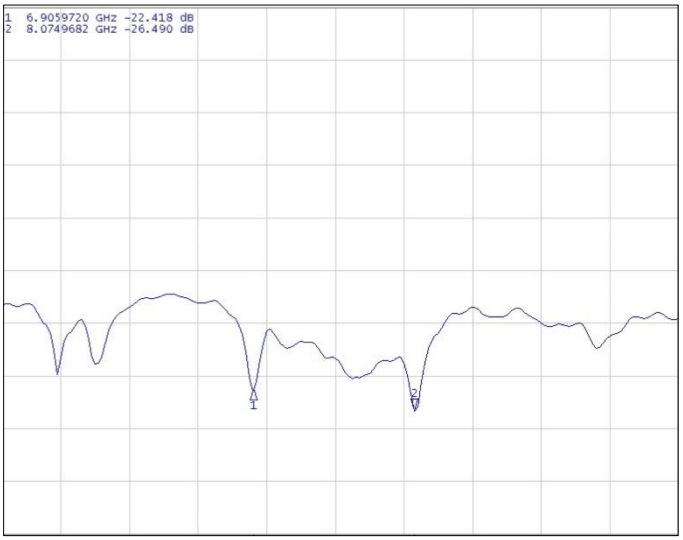

Figure 22: return-loss of fabricated antenna with DRA

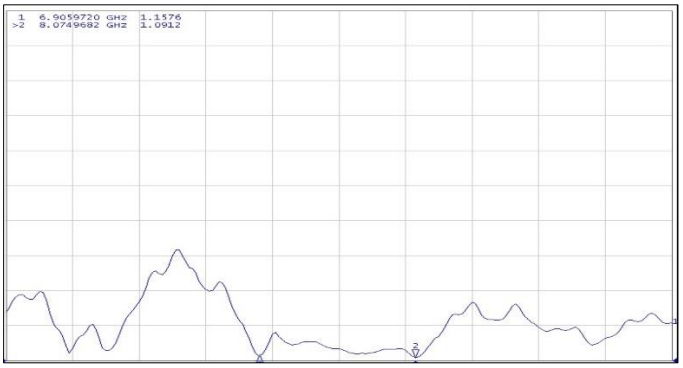

Figure 23: VSWR of fabricated-antenna with DRA

FOREX Publication
Open Access | Rapid and quality publishing
International Journal of Electrical and Electronics Research (IJEER)
Research Article | Volume 11, Special Issue NGWCN | Pages 25-32 | e-ISSN: 2347-470X

5.1 Comparison between simulated and real-world outcomes

The graph below compares the theoretical and actual findings for return loss, VSWR, and gain of a quasi-modified rectangular patch antenna.

Return Loss of with DRA:

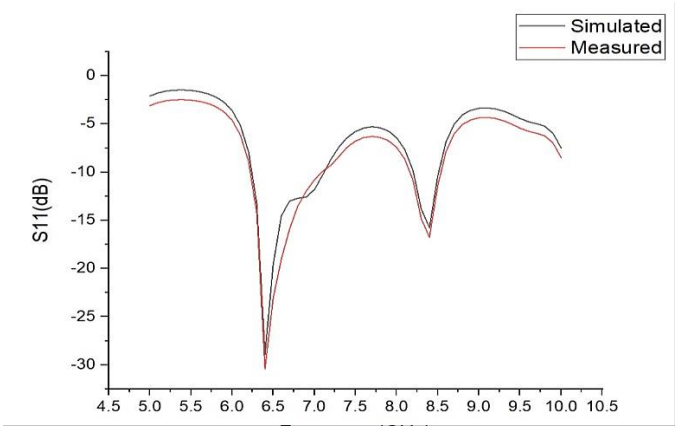

Figure 24: comparison of Return loss for with DRA

VSWR for with DRA:

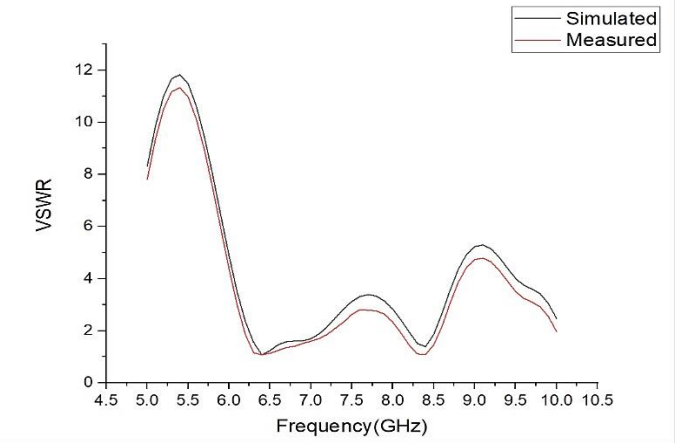

Figure 25: comparison of VSWR for with DRA

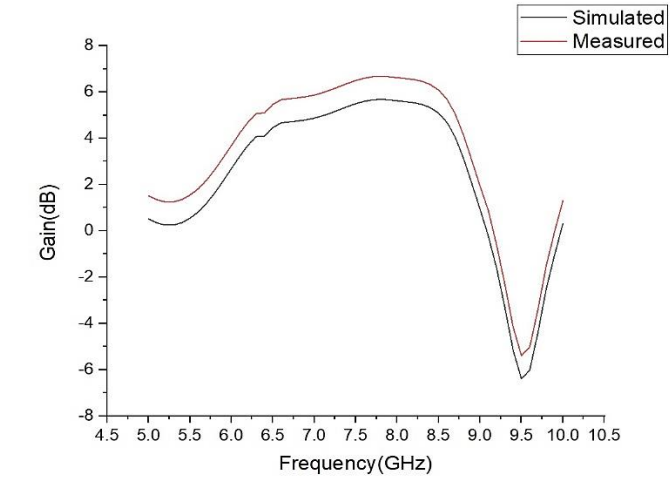

Figure 26: comparison of gain for with DRA

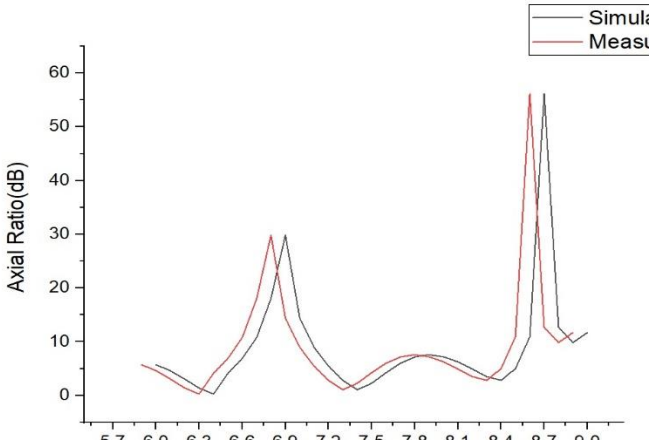

Figure 27: comparison of axial ratio for with DRA

The comparison of the simulated outcomes for the HFSS-coupled, circularly polarized, DRA having fractal slot for all iterations.

Table 3: comparison of above fractal antennas

Iteration Value(n)	"Frequency (GHz)"	"Return Loss(dB)"	"Gain (dB)"	"VSWR"
0(1 Element)	5.4	-15.7504	3.2262	1.3898
1(1 Element)	6.8	-20.1360	4.5320	1.2184
	8.8	-18.2912	4.0857	1.2772
2(1 Element)	6.4	-28.9154	4.1418	1.0743
	8.4	-15.7388	5.8526	1.3904

Table 3 outlines the performance of the circularly polarized DRA with a fractal slot across different iterations, Key metrics like return loss, gain, and VSWR vary across iterations. This data is crucial for designers to identify the best iteration for desired performance in specific applications or frequency bands.

5. MEASURED RESULTS

Figure 20 displays the return-loss curve for the fractal cross-slot antenna without DRA, analyzed by a vector network analyzer. The antenna resonates at 6.79 GHz and 8.26 GHz with return losses of -16.004 dB and -22.64 dB. *Figure 21* shows its VSWR values of 1.32 and 1.17, indicating a well-matched antenna. The VSWR curve for the fractal cross-slot linked antenna without DRA, captured using a vector network analyzer, is displayed in *figures 21 and 23*. *Figure 22* shows the return-loss curve for the fractal cross-slot antenna with DRA, analyzed by a vector network analyzer. It resonates at 6.90 GHz and 8.07 GHz with return losses of -22.41 dB and -26.49 dB. The VSWR values are 1.15 and 1.09.

6. CONCLUSION

The simulation and design of a quasi-modified rectangle patch antenna using the "High-Frequency Structure Simulator (HFSS)" is covered in the article's conclusion. The extensive described and illustrated simulation results show an excellent bandwidth performance, size, radiation patterns, and gain. The antenna operates effectively in the frequency range of 6 GHz

to over 9 GHz, with optimal performance at 6.4 GHz and 8.4 GHz, where the VSWR is less than 2 and the return loss is less than -10 dB. Consequently, this antenna design is well-suited for RADAR and satellite communications applications.

REFERENCES

[1] M. Haneishi and H. Takazawa, "Broadband circularly polarised planar array composed of a pair of dielectric resonator antennas," Electronics Letters, vol. 21, no. 10, pp. 437-438, 1985.
[2] J. Huang, "A technique for an array to generate circular polarization with linearly polarized elements," IEEE Transactions on Antennas and Propagation, vol. 34, no. 9, pp. 1113–1124.
[3] S.-l. S. Yang, R. Chair, A. A. Kishk, K.-F. Lee, and K.-M. Luk, "Study on sequential feeding networks for subarrays of circularly polarized elliptical dielectric resonator antenna," IEEE Transactions on Antennas and Propagation, vol. 55, no. 2, pp. 321–333, 2007.
[4] R.-C. Han, S.-S. Zhong, and J. Liu, "Broadband circularly polarised dielectric resonator antenna fed by wideband switched line coupler," Electronics Letters, vol. 50, no. 10, pp. 725-726, 2014.
[5] K.-W. Khoo, Y.-X. Guo, and L. C. Ong, "Wideband circularly polarized dielectric resonator antenna," IEEE Transactions on Antennas and Propagation, vol. 55, no. 7, pp. 1929–1932, 2007.
[6] G. Massie, M. Caillet, M. Clenet, and Y. M. M. Antar, "A new wideband circularly polarized hybrid dielectric resonator antenna," IEEE Antennas and Wireless Propagation Letters, vol. 9, pp. 347–350, 2010.
[7] M. I. Sulaiman and S. K. Khamas, "A singly fed rectangular dielectric resonator antenna with a wideband circular polarization," IEEE Antennas and Wireless Propagation Letters, vol. 9, pp. 615–618, 2010.
[8] M. Zou, J. Pan, Z. Nie, and P. Li, "A wideband circularly polarized rectangular dielectric resonator antenna excited by a lumped resistively loaded monofilar-spiral-slot," IEEE Antennas and Wireless Propagation Letters, vol. 12, pp. 1646– 1649, 2013.
[9] R. Chair, S. L. S. Yang, A. A. Kishk, K. F. Lee, and K. M. Luk, "Aperture fed wideband circularly polarized rectangular stair shaped dielectric resonator antenna," IEEE Transactions on Antennas and Propagation, vol. 54, no. 4, pp. 1350–1352, 2006.
[10] V. Hamsakutty, A. V. Praveen Kumar, J. Yohannan, and K. T. Mathew, "Coaxial fed hexagonal dielectric resonator antenna for circular polarization," Microwave and Optical Technology Letters, vol. 48, no. 3, pp. 581-582, 2006.
[11] M. Simeoni, R. Cicchetti, A. Yarovoy, and D. Caratelli, "Plastic-based supershaped dielectric resonator antennas for wide-band applications," IEEE Transactions on Antennas and Propagation, vol. 59, no. 12, pp. 4820–4825, 2011.
[12] R. K. Mongia, "Theoretical and experimental resonant frequencies of rectangular dielectric resonators," IEE Proceedings- H, vol. 139, no. 1, pp. 98–104, 1992.